

Crystalline quality and phase purity of CVD diamond films studied by Raman spectroscopy

W. Fortunato · A. J. Chiquito · J. C. Galzerani ·
J. R. Moro

Received: 23 October 2006 / Accepted: 31 January 2007 / Published online: 15 May 2007
© Springer Science+Business Media, LLC 2007

Abstract Two series of diamond films grown—at different temperatures—by two chemical vapor deposition (CVD) methods, i.e., hot filament (HFCVD) and microwave-plasma (MPCVD), were investigated. Raman spectroscopy and scanning electron microscopy were employed to perform a study of both crystalline quality and phase purity of the films grown by the two techniques. It was found that high phase purity can be attained by both methods. However, at high temperatures, the MPCVD technique produced films with higher crystalline quality as compared to those grown by HFCVD. Finally, in order to shed some light into the mechanisms responsible for the lower crystalline quality observed in the HFCVD films, a study based in the phonon confinement model and stress was accomplished.

Introduction

Diamond films grown by chemical vapor deposition (CVD) techniques continue to attract much attention due to their excellent mechanical, physical, chemical and electrical properties [1]. They can be used as coating of mechanical tools, optical windows, microsensors and as a protective layer for integrated circuits. In this study, two of the most common CVD methods used to grow diamond films, the hot filament and the microwave-plasma techniques, were

employed. The diamond lattice exhibits a single characteristic Raman-active mode, the triply-degenerate phonon which appears as a sharp line at approximately $1,332\text{ cm}^{-1}$, considered as a definitive evidence of the diamond presence. The Raman line of natural diamond [2] has a typical width of $\sim 2\text{ cm}^{-1}$ and in polycrystalline CVD diamond films the linewidths are broader (ranging from 5 to 15 cm^{-1}) due to the disorder caused by microstrains or chemical defects. Moreover, the diamond peak is frequently found to be shifted relative to that of natural diamond, due to temperature or lattice strain effects [3]. Under certain growth conditions, various non-diamond carbon structures such as disordered polycrystalline and noncrystalline graphitic carbon regions can be created during the deposition process, leading to poor quality diamond films. Therefore, the analysis of the structural properties of the films, in a variety of growth conditions, can lead to the production of better quality samples.

Many authors have already discussed the quality of CVD diamond films [4–7]. However, to our knowledge, there is no report of an extensive comparative study between the crystalline quality and the phase purity of CVD diamond films grown—as a function of the deposition temperature—by the two techniques here employed, i.e., hot filament (HFCVD) and microwave-plasma (MPCVD). In this work, the study is accomplished by analyzing both the phase purity (here defined as the diamond/graphite Raman spectra ratio) and the crystalline quality (here defined as the Full Width at Half Maximum (FWHM) of the diamond Raman line). Recognizing that the substrate temperature is one of the most important factor affecting the growth process and influencing the diamond film quality, a study was first made on the quality gains (crystalline quality and phase purity), as a function of temperature, for diamond films grown by the HFCVD and

W. Fortunato (✉) · A. J. Chiquito · J. C. Galzerani
Lab de Semicondutores, Departamento de Física, Universidade
Federal de São Carlos, CP 676, São Carlos 13565-905, Brazil
e-mail: pwfs@df.ufscar.br

J. R. Moro
Lab de Diamantes, Universidade São Francisco, Itatiba 13231-
900, Brazil

MPCVD techniques. Then, after observing that for high growth temperatures HFCVD tends to provide films with less crystalline quality as compared to MPCVD, an investigative study based in the phonon confinement model and in the stress was accomplished in the HFCVD sample in order to shed some light into the mechanisms leading to this fact. The films were examined by scanning electron microscopy (SEM) and Raman spectroscopy with special emphasis in the latter technique.

Experimental

Two series of undoped diamond films were prepared, using two different conventional CVD techniques for the activation of the gaseous mixture: hot-filament and microwave plasma reactors. The films were grown on Si(100) wafers (with an area of 1 cm²) metallographically polished. Then, they were treated in an ultrasound bath using a solution of diamond powder with granulometry of 1 μm in hexane during 15 min. In both reactors a gaseous atmosphere composed of 2% CH₄ diluted in H₂ and with a 100 sccm flow rate was used. The gas pressure was kept fixed at 50 torr by a mechanic vacuum pump (E2M8-Edwards). The growth time was kept in 5 h for the hot-filament and in 4 h for the microwave reactor. The substrate holder temperature was measured using cromel-alumel thermocouples. In the first series, six samples were prepared at different deposition temperatures (varying from 508 to 768 °C) using the hot-filament reactor. A tungsten filament (diameter 123 μm) with a 3.8 A current was placed 3 mm above the silicon substrate. In the second series, four samples were prepared at different deposition temperatures (varying from 786 to 906 °C) using the microwave reactor (a commercial microwave generator operating at 2.45 GHz and 1,000 W). Measurements previously realized in our laboratory have shown that the temperature range that provides the best diamond films is different for each technique [8]: from 508 to 768 °C for HFCVD and from 786 to 906 °C range for MPCVD. In this work the same temperature ranges were analyzed and now a comparative study of the diamond qualities obtained with both techniques was accomplished.

The scanning electron microscope (SEM) JEOL JSM-5800LV was used to study the morphology of the film surfaces. All the micrographs were obtained by using secondary electron image (se-SEM). Micro- and macro-Raman spectra were recorded at room temperature using the 5,145 Å line of an Ar⁺ laser. In the former case, we used a true-back-scattering geometry and a microscope objective lens (100×) to focus the incident power (kept at 2 mW) onto the diamond surface with a spot size of about 1 μm. In the latter case, the incident power was kept at

200 mW and the quasi-back-scattering geometry was employed. The scattered light was analyzed using a Jobin Yvon T-64000 triple monochromator supplied with a CCD detector cooled by liquid nitrogen.

Results

Hot filament

Figure 1 shows the Raman spectra of the diamond films grown by hot filament at various deposition temperatures. Figure 1a depicts two broad bands centered at ~1,340 and ~1,600 cm⁻¹ which are, respectively, the so-called D-band (for “disorder-band”) and G-band (for “graphite-band”). Rich-sp² diamond films lead to strong scattering with peaks in these regions [9–11]. The appearance of these lines is the result of the low substrate temperature during the growth process, here $T = 508$ °C. The insertion in Fig. 1 shows that the diamond phase is already present at this temperature. However, although the low-intensity peak at 1,332 cm⁻¹ (insertion in Fig. 1) is an evidence of the diamond phase, the film is practically constituted of disordered amorphous and graphitic carbon structures [11]. In Fig. 1b–f we can observe that as the substrate temperature rises, the Raman spectra clearly show an increase of the diamond peak intensity at ~1,332 cm⁻¹ and a strong decrease of the “non-diamond” band (amorphous carbon and graphitic structures) centered at ~1,520 cm⁻¹. In other words, the diamond film quality has improved in terms of its phase purity. The different phases of carbon existing in the non-diamond band decrease as the deposition temperature increases. This quality gain was evaluated from the

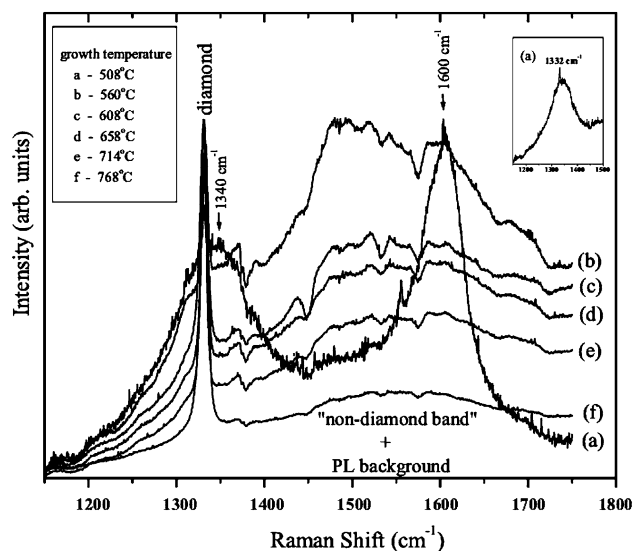


Fig. 1 Raman spectra of the samples grown by the hot filament CVD technique at various deposition temperatures. The insertion shows the initial stage of the diamond grain formation

Raman spectra using a diamond quality factor f_q , which refers to the diamond/graphite ratio, defined as [12]:

$$f_q = \frac{75 \times I_d}{75 \times I_d + \sum_{nd} I_{nd}} \times 100 \tag{1}$$

where I_d is the Raman diamond peak area centered at $1,332\text{ cm}^{-1}$ and $\sum_{nd} I_{nd}$ is the sum of Raman sp^2 phase peak areas. The 75 factor takes into account the more effective Raman scattering of the sp^2 structures [10, 13]. Another accepted criterion for comparing different diamond films is through their crystalline qualities, defined as the full width at half maximum (FWHM) of the first-order Raman peak [1]. This criterion will be also here applied.

Figure 2 shows the dependence of the f_q quality factor, the FWHM values and the position of the diamond Raman peak, on the deposition temperature, for the films grown by both HFCVD and MPCVD techniques. In Fig. 2a (●), the evolution of the calculated quality factor (f_q) for the HFCVD technique shows that almost the diamond phase alone (corresponding to sp^3 bonding) is being grown at high temperatures. As seen in Fig. 2b (●), although an oscillation is observed in the measured FWHM, this parameter attains its largest value when the highest growth

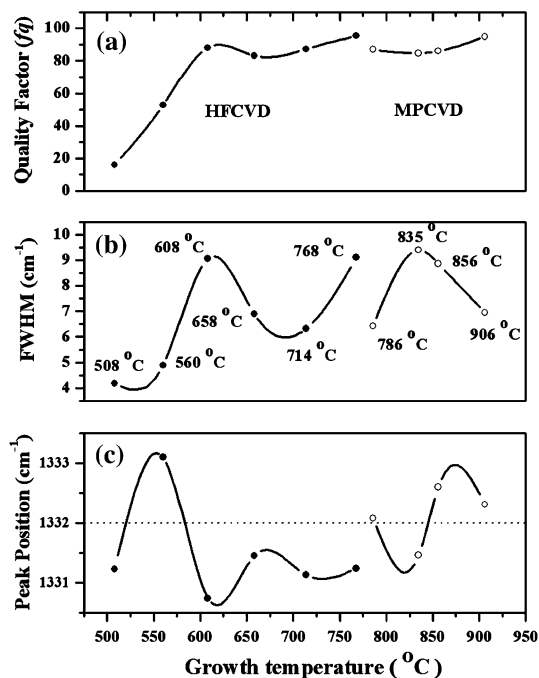


Fig. 2 Quality gain of the diamond films related to (a) the phase purity (f_q), (b) the crystalline quality (FWHM) and (c) the peak frequency, as a function of the growth temperature for both techniques: HFCVD (●) and MPCVD (○). The horizontal dotted line is the position of the natural diamond line. The quality factor f_q was evaluated using the ratio of the area below the diamond peak I_d (with a factor of 75) to the total area of the peaks of the Raman spectrum, excluded the underground. The line was drawn as a guide for the eyes

temperature (768 °C) here used is reached. This result is an indicative that diamond films with poor crystalline quality was grown at that considered temperature. This observation is consistent with that shown in Fig. 2c (●), where the diamond peak position was also observed to oscillate but remaining shifted to a lower frequency (relative to that of natural diamond) indicating the presence of tensile stress in the films. Therefore, considering only our film grown at the highest temperature, the results show that, although this film presents the highest phase purity (Fig. 2a (●)), the crystalline quality is not at its best, as seen in Fig. 2b,c (●).

Microwave

Figure 3 depicts the Raman spectra of the diamond films grown by the microwave technique at different temperatures. The Raman spectra of these films also show decreasing intensities of the non-diamond band as the deposition temperature increases, indicating improved diamond film quality in terms of its phase purity. Figure 2a (○) presents the corresponding f_q quality factor. We can observe that the highest phase purity was obtained for a substrate temperature of $T = 906\text{ °C}$. Thus, this technique also provides diamond films with good phase purity, but at higher temperatures than the hot filament one, as we can see in Figs. 2a (●) and (○). In Fig. 2b (○), the evolution of the measured FWHM with the temperature exhibits an anticorrelation as compared to that observed for HFCVD. Contrary to that, this parameter attains its smallest value when the highest growth temperature (906 °C) here used is reached. This observation is also consistent with that of Fig. 2c (○), where the diamond peak position is also observed to oscillate with temperature but remaining (in the

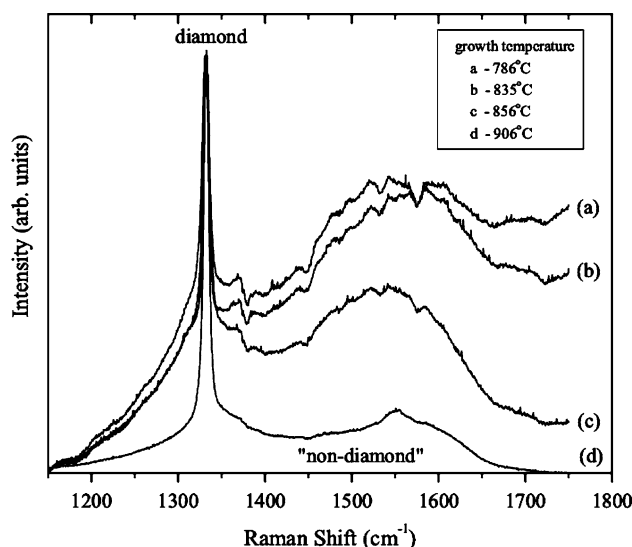


Fig. 3 Raman spectra of the samples grown by microwave CVD technique at various deposition temperatures

average) close to that of the natural diamond. This suggests that the present films are nearly stress free, in contrast to that observed for HFCVD. Therefore, the film grown at the highest temperature with MPCVD is found to provide not only the highest phase purity (Fig. 2a (○)) but also the best crystalline quality, as shown in Fig. 2b,c (○).

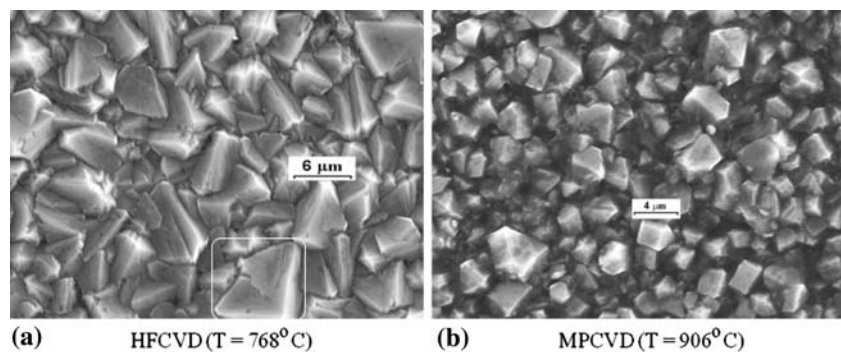
Discussion

HFCVD versus MPCVD diamond films

As observed in the Raman spectra of Figs. 1f and 3d, the samples grown at the highest temperatures by HFCVD and MPCVD techniques showed, respectively, the highest quality among the films here obtained. However, the SEM images depicted in Fig. 4 show a rather visible difference between their crystalline morphology. Although some evidence of polycrystalline diamond films with morphology dominated by $\langle 111 \rangle$ and $\langle 220 \rangle$ -faceted crystallites was observed in both kinds of samples, the average grain size was found to be larger ($\sim 6 \mu\text{m}$) and defective in the HFCVD film (see Fig. 4a) in comparison to the smaller ($\sim 4 \mu\text{m}$) and well-faceted in the MPCVD (see Fig. 4b). The observations above mentioned are in a good agreement with the results shown in Fig. 2. As we can observe in Fig. 2a (●) and (○), both HFCVD and MPCVD produce diamond films with equivalent phase purity. Both techniques exhibit considerable reduction of the non-diamond Raman band leading to quality gain factors of approximately the same value ($f_q \approx 95$). However, considering the FWHM's of the same high temperature samples (Fig. 2b (●) and (○)) the films grown by MPCVD presented the smaller value. This result indicates that the crystalline quality is better for the MPCVD technique, justifying the SEM image shown in Fig. 4b. In Fig. 4a, most of the cracks appears mainly inside the grains of that HFCVD film and propagates along the edges between facets, indicating that a large strain was induced in that film. Much probably, this effect is the responsible for the larger

FWHM value (line broadening) and peak frequency shifts shown, respectively, in Fig. 2b,c (●). Thomas S. MacCaulley and Yogesh K. Vohra [14] point out two possible causes for the line broadening: the residual internal strain (caused by the substrate and the grain boundary mismatch within the films), and the relaxation of the $\mathbf{k} = 0$ wave-vector selection rule for Raman scattering due to the formation of finite-sized crystalline domains during the growth. According to Nemanich, Solin, and Martin [15], and Fauchet and Campbell [16] the grain size must be less than $10^{-2} \mu\text{m}$ for a significant grain size effect to be observed in the Raman spectrum of a film. Since the average grain size of our best quality diamond films grown by both techniques exceeds $1 \mu\text{m}$ (Fig. 4a,b), the residual internal strain appears to be the primary broadening mechanism in the diamond films here studied. Therefore, in order to verify if such a mechanism is responsible for the broadening of the Raman lines in our films, micro-Raman analysis was performed in the samples shown in Fig. 4a,b. Micro-Raman spectra taken from several grains of MPCVD film (not shown here) did not show any asymmetry. Moreover, the spectra revealed a smaller contribution to the broadening and shifts to higher frequency than that observed in the samples grown by HFCVD. In opposition, micro-Raman spectra obtained from several grains of the HFCVD film depicted in Fig. 4a showed strongly asymmetric line shapes, which is a characteristic of the particle size. Because of this, the analysis of such mechanism was performed on the film grown by hot filament alone. Raman spectra taken in three different grains (a, b and c) are depicted in Fig. 5. The observed asymmetry was not expected since these Raman spectra were taken from large grains ($>10^{-2} \mu\text{m}$), like those appearing in the SEM images shown in Fig. 4a. However, a plausible argument for the observed result is that it is an indication of defects of some sort inside each grain, which effectively confine the phonons to subgrain regions. Thus, the asymmetric broadening towards the lower frequencies observed in Fig. 5 can be explained using a phonon-confinement model [17].

Fig. 4 The secondary electron SEM images of the diamond films grown at the highest temperatures for each CVD technique here studied: (a) hot filament (HFCVD) and (b) microwave plasma (MPCVD). The region enclosed by the rectangle is that which contains the grain zoomed on in Fig. 7



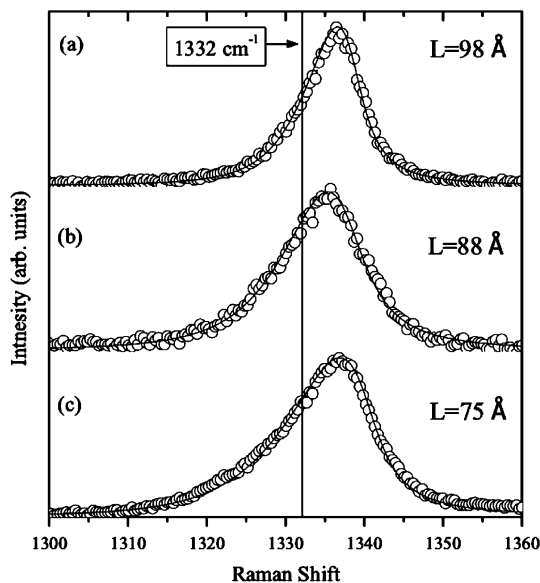


Fig. 5 Raman spectra of three different grains of the best-quality sample grown by hot filament. The *circles* and *continuous lines* are the experimental and theoretical results, respectively. The *vertical line* is the position of the natural diamond line

Phonon-confinement model

According to the phonon-confinement model [17,18], a Raman line shape may be calculated by superimposing a group of Lorentzian line shapes centered at (q) , weighted by the uncertainty in wave-vector q caused by the confinement:

$$I(\omega) \cong \int_0^1 \frac{\exp(-q^2 L^2/4) 4\pi q^2 dq}{[\omega - \omega(q)]^2 + (\Gamma_0/2)^2}, \tag{2}$$

where q is an approximate one-dimensional phonon dispersion curve, q is expressed in units of $2\pi/a$, L is the crystallite size in units of a (3.567 Å), the lattice constant of diamond, and Γ_0 is the natural linewidth. For the dispersion curve $\omega(q)$, we assumed the form [3, 19]:

$$\omega(q) = A + B \cos(q\pi), \tag{3}$$

where $A = 1,241.25 \text{ cm}^{-1}$ and $B = 91.25 \text{ cm}^{-1}$.

The result for the three grains a, b and c, corresponding to the Raman spectra shown in Fig. 5, were calculated using the phonon confinement model by Eqs. 2 and 3 and values the of $L = 98, 88$ and 75 Å were found. As we can see in Fig. 5, the curves fitted with the confinement model are in good agreement with the experiment. However, a shift in the calculated curves had to be introduced in order to obtain a good fitting with the experimental data. The disagreement between the observed (Fig. 5) and the calculated line shapes, for the same values of L , can be clearly

seen in Fig. 6. The central positions of the diamond line shapes in Fig. 5 appear shifted to higher frequencies than that of the natural diamond at $1,332 \text{ cm}^{-1}$, while in the predicted line shape calculated by the phonon-confinement model (Fig. 6) they are shifted to lower frequencies. Because of this lack of agreement between the observed and predicted shapes, we believe that the mechanism for the observed asymmetry, broadening and shifts to higher frequencies in the Raman spectra of this film cannot be explained by the phonon-confinement model alone. The shift of the diamond Raman line to higher frequencies appears to be due to a compressive stress caused by a residual strain in the films. Such a conclusion is in agreement with the grain shape enclosed by a rectangle in the SEM images shown in Fig. 4a.

Influence of stress

In order to verify the influence of the mechanical stress as another mechanism responsible for the broadening and frequency shifts of the Raman lines, micro-Raman spectra were taken from three different regions (1, 2 and 3) of that defective grain surface observed in Fig. 4a. The results are depicted in Fig. 7. The Raman spectra clearly showed the presence of residual compressive (1 and 2) and tensile (3) stresses, even within a single grain. The Raman shift is known to be proportional to the bi-axial stress in the diamond films, as follows [20]:

$$\sigma = -1.08(v_s - v_0) \text{ (GPa)} \text{ for a singlet phonon,} \tag{4}$$

$$\sigma = -9.384(v_d - v_0) \text{ (GPa)} \text{ for a doublet phonon,} \tag{5}$$

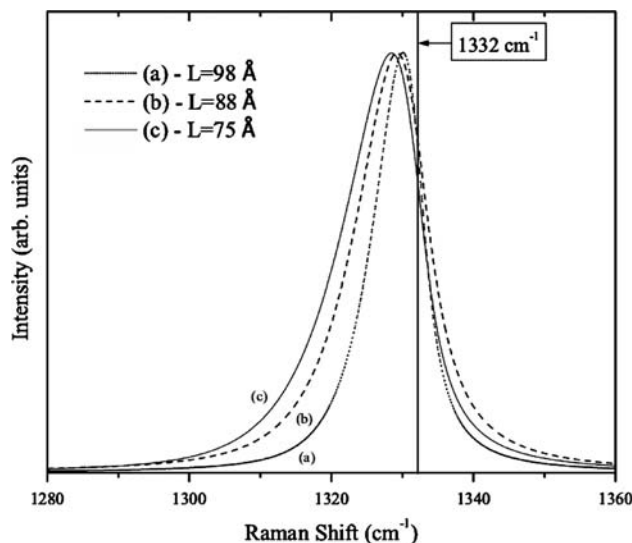


Fig. 6 Calculated Raman line shapes of the diamond particles with sizes of 98, 88 and 75 Å. The *vertical line* is the position of the natural diamond line

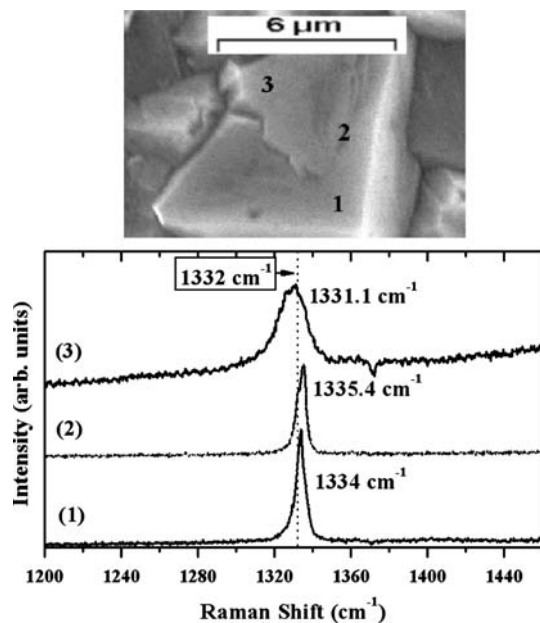


Fig. 7 The secondary electron SEM image and the micro-Raman spectra of a defective grain observed in Fig. 4a, clearly showing the presence of the residual stresses in the film: compressive (1) and (2) and tensile (3) stress. The numbers 1, 2 and 3 show the three regions with different stresses. The vertical dotted line is the Raman line of natural diamond

where $\nu_0 = 1332 \text{ cm}^{-1}$, ν_s is the observed maximum of the singlet in the spectrum and ν_d the maximum of the doublet. In many films, the splitting of the Raman line is not obvious. In this case, the observed peak position ν_m is assumed to be located at the center between the singlet ν_s and doublet ν_d , i.e., $\nu_m = (1/2)(\nu_s + \nu_d)$ [21]. From Eqs. 4 and 5 we obtain

$$\sigma = -0.567(\nu_m - \nu_0) \text{ (GPa)}, \quad (6)$$

where $\sigma < 0$ and $\sigma > 0$ correspond to the compressive and tensile stress, respectively. As shown in Fig. 7 (1, 2 and 3), no splitting was observed. We then used Eq. 6 in order to calculate the residual stress in the film and the values found are shown in Table 1. It is now possible to infer that both phonon confinement and residual stress are responsible for the observed asymmetry, broadening and shifts to higher frequencies in the Raman line.

Table 1 Stress calculation in a single grain of a film grown by HFCVD

Regions	ν_m	σ (GPa)	Type of stress
1	$1,334.0 \text{ cm}^{-1}$	-1.13	Compressive ($\sigma < 0$)
2	$1,335.4 \text{ cm}^{-1}$	-1.91	Compressive ($\sigma < 0$)
3	$1,331.1 \text{ cm}^{-1}$	0.51	Tensile ($\sigma < 0$)

The numbers 1, 2 and 3 correspond to the different regions chosen on the grain as shown in Fig. 7

Conclusions

Using the phase purity and the crystallinity as parameters to analyze and compare the quality of the diamond films, we concluded that both growth techniques (HFCVD and MPCVD) produce diamond films of similarly good purity; however, the largest purity of the films could be attained at a lower temperature ($T = 768 \text{ }^\circ\text{C}$) for HFCVD as compared to MPCVD ($T = 906 \text{ }^\circ\text{C}$). On the other hand, MPCVD produces diamond films with better crystallinity. Micro-Raman spectra obtained from grains of the diamond film grown by HFCVD with the highest quality shows that the mechanism for the observed asymmetry, broadening and shifts to higher frequencies in the Raman line cannot be fully explained by the phonon-confinement model. Residual stresses must be considered. We then propose that such mechanism for the observed line shapes in the Raman spectra of films grown by the HFCVD technique is a result of the presence of both confinement and residual stresses in the films, occurring even in a single grain.

Acknowledgements The author (W.F) would like to thank Dr. Paulo Sergio Pizani for useful discussions. This work was partially supported by the Brazilian agencies, CAPES, CNPq and FAPESP.

References

- Clark CD, Mitchell EW, Parsons BJ (1979) In: Field J (ed) The properties of diamond. Academic, London, p. 23
- Solin SA, Ramdas AK (1970) Phys Rev B 1:1687
- Ager JW III, Veirs DK, Rosenblatt GM (1991) Phys Rev B 43:6491
- Yoshikawa M, Katagiri G, Ishida H, Ishitani A, Ono M, Matsumura K (1989) Appl Phys Lett 55:2608
- Donato MG, Faggio G, Marinelli M, Messina G, Milani E, Paoletti A, Santangelo S, Tucciarone A, Rinati GV (2001) Eur Phys J B 20:133
- Grus M, Jankowska-Frydel A, Bohdanowicz J, Zawada K (2001) Cryst Res Technol 36:961
- Fayette L, Marcus B, Mermoux M, Tourillon G, Laffon K, Parent P, Le Normand F (1998) Phys Rev B 57:14123
- Fortunato W, Chiquito AJ, Galzerani JC, Moro JR (2005) Thin Solid Films 476:246
- Gogotsi YG, Per Kofstad, Yoshimura M, Nickel KG (1996) Diamond Relat Mater 5:151
- Shroder RE, Nemanich RJ, Glass JT (1990) Phys Rev B 41:3738
- Knight DS, White WB (1989) J Mater Res 4:385
- Silva F, Gicquel A, Tardieu A, Cledat P, Chauveau T (1996) Diamond Rel Mater 5:338
- Wada N, Solin SA (1981) Physica B C 105:353
- MacCauley TS, Vohra YK (1994) Phys Rev B 49:5046
- Nemanich RJ, Solin SA, Martin RM (1981) Phys Rev B 23:6348
- Faucher PM, Campbell IH (1988) Crit Rev Solid State Mater Sci 14:S79
- Richter H, Wang ZP, Ley L (1981) Solid State Comm 39:625
- Campbell IH, Faucher PM (1986) Solid State Comm 58:739
- Tiong KK, Amirtharaj PM, Pollack FH, Aspnes DE (1984) Appl Phys Lett 44:122
- Ager JW III, Drory MD (1993) Phys Rev B 48:2601
- Ralchenko VG, Smolin AA, Pereverzev VG (1995) Diamond Relat Mater 4:754